Research Article Available online www.ijsrr.org ISSN: 2279–0543

International Journal of Scientific Research and Reviews

Electrical conductivity of diene and pheneMolecular Nanowires: A QTAIM approach

JothiB.[1], Stephen A. David[2], Palanisamy S.[1] and Selvaraju K.*[1]

[1]Department of Physics, Kandaswami Kandar's College, Velur, Tamilnadu, India – 638182
[2]Dept.ofPhysics,PSG college of Arts and Science, Coimbatore, Tamilnadu, India- 641014
DOI - http://doi.org/10.37794/IJSRR.2023.12302

ABSTRACT

The impact of electric field (EF) in a proposed nanowires diene and phene has been examined hypotheticallyfrom the basic and electronic charge transport properties utilizing the first principles of quantum calculations and QTAIM theory. The applied EF (0–0.26VÅ-1) modifies the molecular confirmation, electron density, electrostatic properties and the orbital levels of the molecule. Moreover, the applied EF alters the homo-lumo gap, which reveals the nature of the electrical conductivity. The electrostatic potential for different degrees of applied EF uncovers the charge concentration of the molecule. The I–V qualities of the molecule have been considered against different applied fields utilizing Landauer formalism

KEYWORDS: Nanoelectronics; QuantumCalculations; QTAIMtheory; I-Characteristics

***CorrespondingAuthor:**

K.Selvaraju

Assistant Professor and Head, Department of Physics,

Kandaswami Kandar's College,Velur-638182

Tamilnadu, India. Email: physicsselvaraj@gmail.com

Mobile:9442430003

INTRODUCTION

When the molecule is fused between the metal terminals, electron flow from one side to the other was occurred. This electron flow produces the current stream the other way. Electron transfer is the most straightforward response, and one in which no chemical bonds are created nordestroyed[1]. This phenomenon was also observed in other common process, including photosynthesis, and is firmly identified with the course of molecular structure. Subsequently, the investigation of molecular structures and the electron transport through them stays critical. Transport phenomena through molecular layers ought to be considered and investigated seriously, since they trace a wide scope of operations in sub-atomic level research. In this connection, we carried out the theoretical investigation of electrical conductivity of diene and phene (Fig 1), from high level quantum chemical calculations.

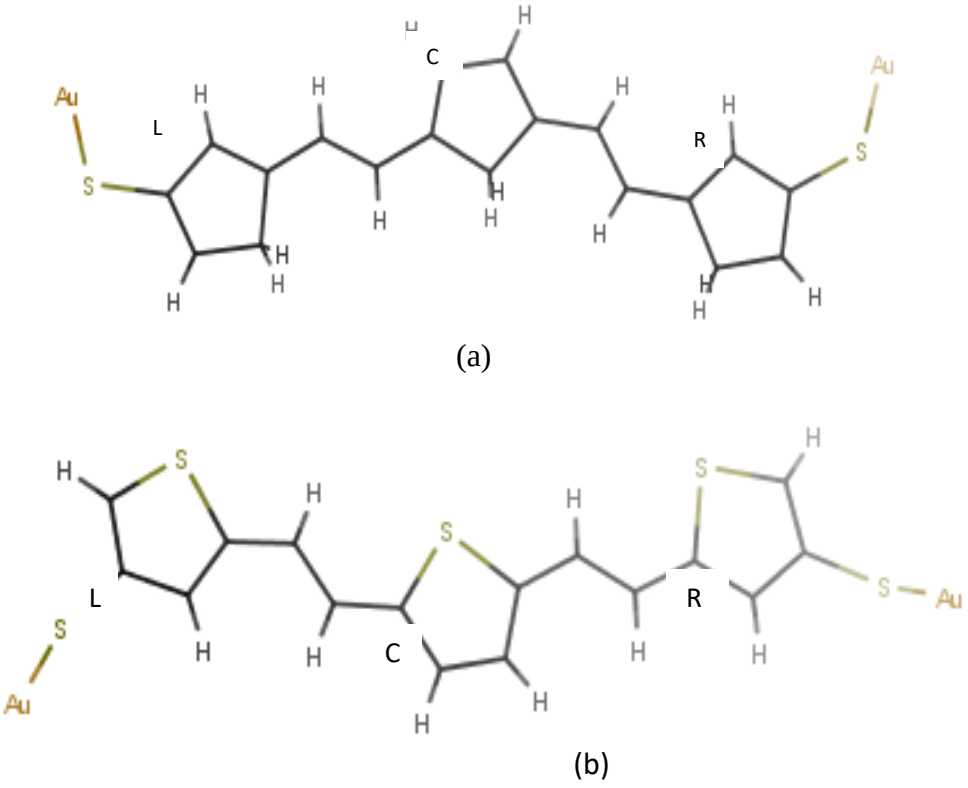

Fig. 1. Schematic diagram of (a) diene and (b) phene fused with Sulphur and Gold atoms.

It is yet challenged to comprehend the charge transport mechanism of metal–molecule junction tentatively; this difficulty emerges because of a few sorts of experimental factors that

influence the resulting information. To overcome this,the first principle of quantum mechanics and electron density analysis have been utilized to relate the charge transport properties all the more decisively with the electrode-molecule junction. In the present investigation, we have dissected the electrical conductivity of diene and phene for different levels of applied electric field (EF) based on electron/energy density analysisvia high level quantum calculation combined with AIMhypothesis[2]. The I–V characteristics of the diene and phenemolecular wires have also been investigated for different applied fields.

Computational details

The geometry of diene and phene along with the electrodes was optimized for the zero and higher applied electric fields ranges from 0VÅ^{-1} to 0.26VÅ^{-1} from density functional theory [DFT][3] strategy coupled in Gaussian03 program[4]. In this regard, Becke's three-parameter exchange function with non-local correlation of Lee, Yang and Parr (B3LYP hybrid function)[5]is used along with Los Alamos National Laboratory of double zeta basis set [LANL2DZ][6,7], as it conveys the total clarification of overwhelming metal atoms, Sulphur and Gold. The atomic charges are calculated from different algorithms, MPA[8] and NPA[9].

The energy minimization was assessed through Berny calculation and the calculation is saturated with the threshold values of 0.00045, 0.0003, 0.0018 and 0.0012au for the maximum force, root mean square force (RMS), maximum displacement and RMS displacement respectively. In this study, all the quantum calculation was completed for various degrees of applied electric field to observe the difference in the geometry compliance, chemical bond qualities and the electrostatic properties of the diene and phene molecular nanowires. The bond topological and the electrostatic properties have been anticipated from the QTAIM hypothesis by means of EXT94b module executed in the AIMPAC programming[10]. DENPROP[11]and wfn2plots[12] were utilized to create two dimensional matrices for mapping the Laplacian of electron density and the static deformation density. The GVIEW[13] was utilized to investigate the three-dimensional surface plots. The density of states (DOS) for various applied EFs was all around encircled from the Gauss Sum program[14].The quantitative molecular electrostatic potential map for both experimental and predicted crystal structures was generated and visualized on the three-dimensional surface using the program WFA-SA[15].

Results and Discussion

Structural aspects

The overlap of geometrically minimized structures of gold and sulphurattacheddiene and phene molecular wire for zero and applied electric field are pictured in the figure 2.

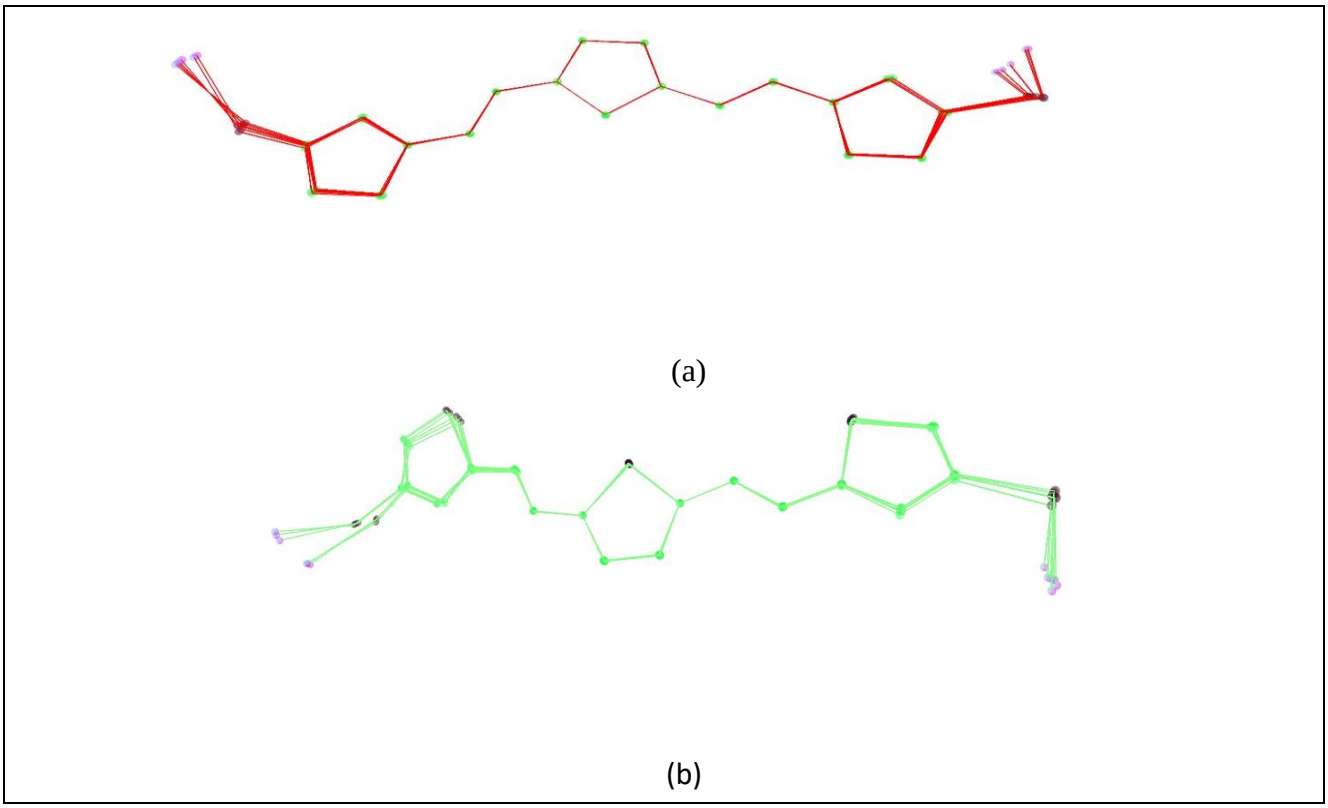

Fig. 2Superimpose of the Au & S substituted (a) dieneand (b) phene for the zero and various applied EFs.

The molecular orientation is not exactly same on the two edges (right and left) of the molecule and found a less difference under the influence of the electric field. The bond length of both the molecule for the zero and non-zero electric field was listed in the supplementary table 1. For the diene molecule, the average C−C bond distances in all the three 5-memebered rings for the zero applied field is ~1.453 Å and this was found to increase slightly by ~0.0005 Å when the electric field is increased from 0 to 0.26VÅ^{-1}. The maximum difference [~0.0054 Å] in C-C bond distance was noticed for the bonds connected with the bridge bonds between the rings of the molecule. The S−C bond distance is ~1.818 Å for the 0ev and this value agree well with the reported theoretical [7,13] and experimental data [14]. At the point when the field is extended from 0.05 to 0.26VÅ^{-1}, the S-C bond getting extended from 1,818 Å to 1.820 Å in left edge, while in the right edge, no such difference was noted upon the application of electric field. Among the bonds, S-Au bonds are highly influenced by the applied electric field with the maximum deviation of about 0.02 Å. The Au−S bond distance

in left and right closures are 2.404 Å, for zero applied electric field which was well concur with the reported [15, 16]values. When the electric field is increased, this distance gets shortened (2.398Å) in the left side, conversely the equivalent was expanded (2.414Å) in the right side. Asphene molecule is having sulphur replacement in five member edrings, the bond distance is varied drastically when compared with that of diene molecule, which was shown in the figure 3. The bond distance of C-C bonds [~1.403Å] in these rings was shortened by 0.05 Å when compared with that of same in diene molecule and this attribute the presence of sulphur atom in the five membered rings. The C-S bond distance in the five membered rings for zero electric field is ~1.812 Å, and this was slightly increased by ~0.02 Å when the electric field is increased from 0 to 0.26VÅ^{-1}. In diene molecule, the terminal bond angle Au−S−C at the left was increased weakly by ~1° [102 to 103°] and at the right edge, the same angle was increased by same difference with the applied electric field. The scenario is contrast for phene molecule, and it was noticed that the Au−S−C bond angle was decreased at the left and increased at the right with the applied electric field. The dihedral angle, Au−S−C−C bonds, both at right and left edges, was absolutely decreased from -66.8° to -61.3° [diene] and -79.7° to -74.1° [phene] as theapplied electric field increased from 0 to 0.26 VÅ^{-1}.

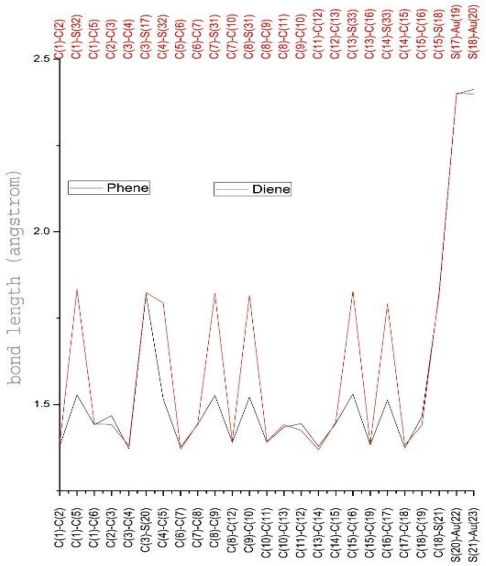

Fig. 3Variation of average bond length of diene and phenemolecule.

CHARGE DENSITY AND LAPLACIAN OF ELECTRON DENSITY

The electron density analysis and their topological properties were characterized on the basis of Quantum theory of Atoms in Molecule theory proven by Bader[16]. For the zero and non-zero applied electric field, the 2D contour plots posing the dynamic deformation density in the molecular plane was exhibited from the figure 4. For Diene molecule, like the reported data, the average value of electron density for zero applied electric field at the bond critical point in C-C bonds of all the

three 5-membered rings is ~1.63eÅ^{-3}. This value was slightly lower than the C=C bond densities whose average value is ~2.03 eÅ^{-3}. Remarkably, when the applied electric field increases, the C-C bond densities are found to be increased by 0.01eÅ^{-3} and C=C densities are decreased by same value. Interestingly, the variation of C–C and C=C bond densities $\rho_{bcp}(r)$ are systematic for the applied electric fields. The C=C bond density is significantly high, when compared with all other bonds in the molecule which directs that the charges of these bonds are highly accumulated and are migrated towards the inter-nuclear axis. This trend can be well reflected from the Laplacian of electron density [17] values. The S−C bond density in the left and right region at the zero electric field establishes its ionic nature, whereas the average $\rho_{bcp}(r)$ value is 1.042 eÅ^{-3}.On increasing the electric field, the S-C bond density is decreased to ~1.039 eÅ^{-3}. The Au−S bond density in the terminal region at left and right ends are 0.52 eÅ^{-3} for the zero-bias situation; as the field increases, these density values were differing by +0.009 eÅ^{-3} and -0.017eÅ^{-3}in both the ends respectively. As for as Phene molecule concern, the average C-C and C=C bond electron density for zero applied electric field is 1.83 eÅ^{-3}and 1.99 eÅ^{-3}respectively and there is no significant variation was noticed upon the increase of electric field. The C-S bond density in ring and terminal regions at zero electric field are ~1.08eÅ^{-3}and ~1.03eÅ^{-3}respectively, and the same was reduced by 0.01eÅ^{-3}when the field increased from 0 to 0.26VÅ^{-1}. The entire spectrum of electron density $\rho_{bcp}(r)$ are posed in Table 1.

The Laplacian of electron density $[\nabla^2\rho_{bcp}(r)]$, has been raised from second order partial derivative of electron density, which quantifies the curvature of the function in 3D. The negative value of Laplacian directs to the locally concentrated charges at the bcp and a positive value lead to the locally depleted. The covalent nature of these bond C−C and C=C bonds was well confirmed from the negative Laplacian of electron density values and exhibiting an *open-shell* interaction[18]. The $\nabla^2\rho_{bcp}(r)$ values at the bond critical point of C-C and C=C bonds in diene/phene molecules are calculated as -12.6/-16.1eÅ^{-5} and -19.4/-18.5eÅ^{-5} respectively. This difference may be attributed towards the presence of Sulphur in the five membered rings of phene molecule. The average $\nabla^2\rho_{bcp}(r)$ value of (C-S) ring bond intthephene molecule is~-4.8eÅ^{-5}. When field increases, the negative Laplacian values of left region S-C bonds are found to bedecreased at both the edges, the value ranges from -4.70 to -4.67eÅ^{-5} at the left edge and from -4.67 to -4.62eÅ^{-5}at the right. The same trend was noticed for Phene, with values decreased from -4.52 to -4.43eÅ^{-5}and from -4.52 to -4.39 eÅ^{-5}at the left and right edge respectively. The *closed-shell* type Au-S interaction[19] was evident from the positive values of Laplacian [3.16 eÅ^{-5}]. Supplementary, it is observed that the charges of these bonds are well exhausted for the aggregated electric field, this charge delocalization can be

envisaged from the Laplacian of electron density two-dimensional contour plots (Fig. 6). The Laplacian of electron density values of Au−S bond in the left region differs from 2.95 to 3.16 eÅ^{-5},

whereas in the right region, this value ranges from 2.96 to 3.06 eÅ^{-5}for higher field [0 - 0.26 VÅ^{-1}]. Similar pattern was observed for phene molecule. The deviation in Fig 5b spectacles the Sulphur atom replacement. The $\nabla^2\rho_{bcp}(r)$ values are listed in table 2

EF(VÅ^{-1})	Deformationdensity
0.0	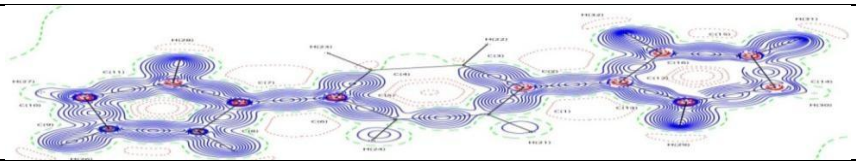
0.05	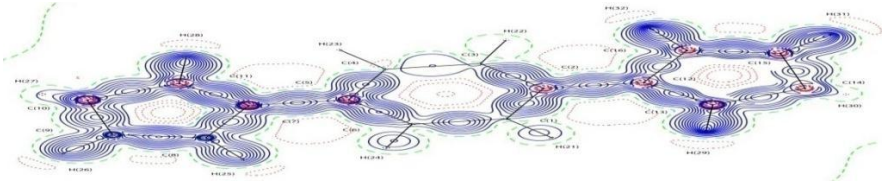
0.10	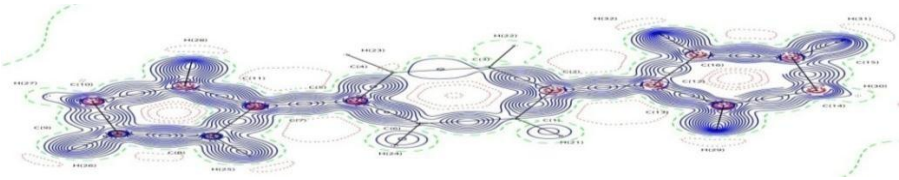
0.15	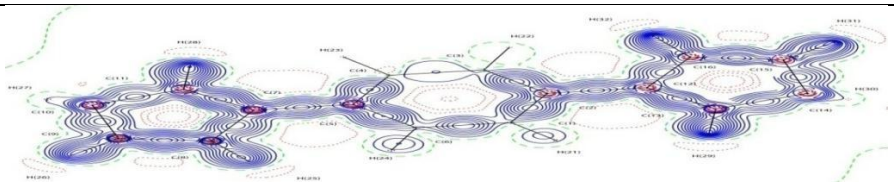
0.21	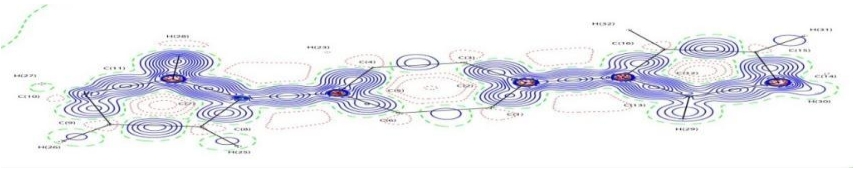
0.26	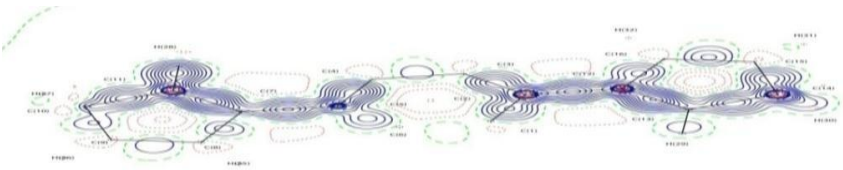

Fig. 4 Deformation density map plotted for molecular plane of (a) diene and (b) phene for the zero and0.26 applied EFs.Solid lines represent positive contours, dotted lines are negative contours and dashed lines are zero contours. The contours are drawn at 0.05 eÅ^{-3} intervals.

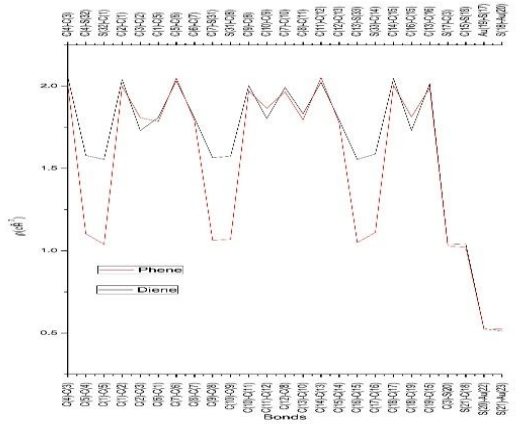

(a)

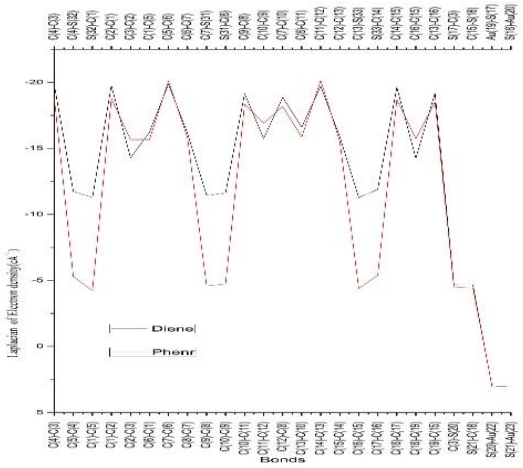

(b)

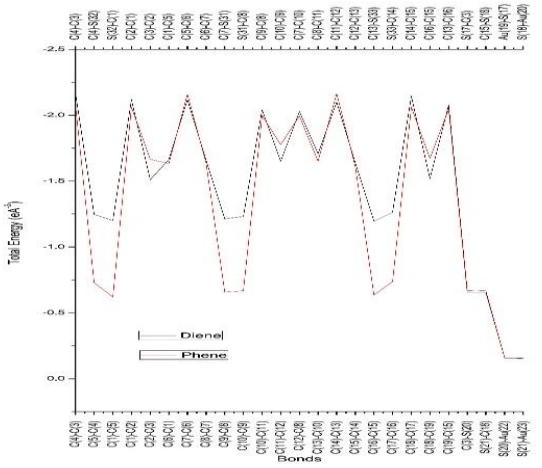

(c)

Fig. 5Average (a) Electron density,(b) Laplacian of electron density and (c) total energy variation of diene and phene.

Table 1 Electron density $\rho_{bcp}(r)$ ($eÅ^{-3}$) values of the diene and phene wire for the various applied EFs ($VÅ^{-1}$).

Bonds	0	0.05	0.1	0.18	0.21	0.26
C (4)-C (3)	2.055	2.056	2.057	2.057	2.054	2.052
C (5)-C (4)	1.58	1.579	1.578	1.578	1.578	1.579
C (1)-C (5)	1.553	1.554	1.554	1.555	1.556	1.557
C (1)-C (2)	2.039	2.04	2.041	2.04	2.038	2.034
C (2)-C (3)	1.728	1.728	1.728	1.729	1.731	1.735
C (6)-C (1)	1.803	1.804	1.806	1.81	1.814	1.821
C (7)-C (6)	2.037	2.037	2.036	2.033	2.029	2.022
C (8)-C (7)	1.799	1.799	1.801	1.805	1.811	1.819
C (9)-C (8)	1.564	1.565	1.565	1.565	1.565	1.566
C (10)-C (9)	1.573	1.574	1.574	1.574	1.573	1.573
C (10)-C (11)	2.01	2.01	2.007	2.002	1.996	1.988
C (11)-C (12)	1.792	1.793	1.797	1.803	1.81	1.82
C (12)-C (8)	2	1.999	1.996	1.992	1.986	1.978
C (13)-C (10)	1.819	1.822	1.827	1.834	1.841	1.849
C (14)-C (13)	2.036	2.033	2.029	2.022	2.015	2.006
C (15)-C (14)	1.784	1.786	1.789	1.794	1.8	1.806
C (16)-C (15)	1.559	1.557	1.556	1.554	1.552	1.55
C (17)-C (16)	1.591	1.59	1.588	1.587	1.585	1.585
C (18)-C (17)	2.05	2.049	2.047	2.045	2.043	2.042
C (18)-C (19)	1.73	1.729	1.73	1.731	1.732	1.732
C (19)-C (15)	2.025	2.022	2.018	2.013	2.007	2
C (3)-S (20)	1.043	1.04	1.038	1.036	1.035	1.034
S (21)-C (18)	1.042	1.043	1.043	1.042	1.041	1.04
S(20)-Au (22)	0.52	0.522	0.525	0.528	0.528	0.529
S(21)-Au(23)	0.52	0.518	0.516	0.514	0.51	0.503

Bonds	0	0.05	0.1	0.18	0.21	0.26
C (4)-C (3)	2.007	2.008	2.008	2.009	2.009	2.009
C (4)-S (32)	1.109	1.106	1.104	1.103	1.099	1.096
S (32)-C (1)	1.045	1.043	1.04	1.038	1.036	1.034
C (2)-C (1)	2	2.001	2	1.999	1.998	1.997
C (3)-C (2)	1.81	1.809	1.808	1.807	1.807	1.807
C (1)-C (5)	1.787	1.786	1.785	1.784	1.784	1.784
C (5)-C (6)	2.052	2.052	2.05	2.049	2.047	2.045
C (6)-C (7)	1.785	1.787	1.789	1.791	1.794	1.797
C (7)-S (31)	1.067	1.066	1.064	1.063	1.062	1.06
S (31)-C (8)	1.071	1.071	1.07	1.07	1.068	1.067
C (9)-C (8)	1.97	1.97	1.97	1.97	1.97	1.969
C (10)-C (9)	1.864	1.864	1.865	1.865	1.866	1.868
C (7)-C (10)	1.965	1.966	1.966	1.966	1.965	1.964
C (8)-C (11)	1.798	1.797	1.796	1.794	1.794	1.794
C (11)-C (12)	2.052	2.053	2.053	2.053	2.052	2.051
C (12)-C (13)	1.773	1.774	1.775	1.775	1.777	1.779
C (13)-S (33)	1.052	1.052	1.051	1.05	1.049	1.049
S (33)-C (14)	1.117	1.114	1.112	1.108	1.106	1.104
C (14)-C (15)	2	2.002	2.004	2.005	2.006	2.007
C (16)-C (15)	1.814	1.814	1.814	1.812	1.812	1.812
C (13)-C (16)	1.989	1.989	1.989	1.99	1.989	1.989
S (17)-C (3)	1.029	1.029	1.029	1.028	1.027	1.024
C (15)-S (18)	1.029	1.026	1.023	1.021	1.018	1.016
Au(19)-S (17)	0.521	0.521	0.521	0.521	0.524	0.523
S(18)-Au(20)	0.521	0.522	0.524	0.527	0.527	0.527

EF($VÅ^{-1}$)	Laplacian of electron density
0.0	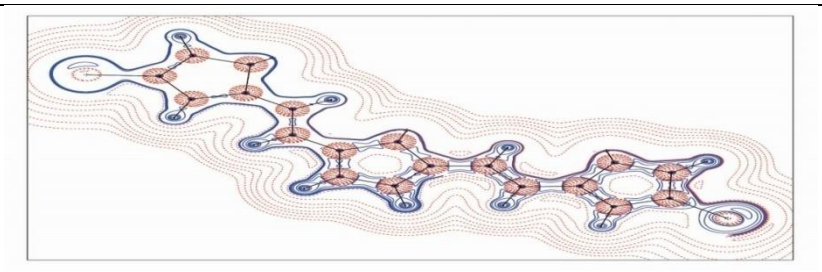
0.26	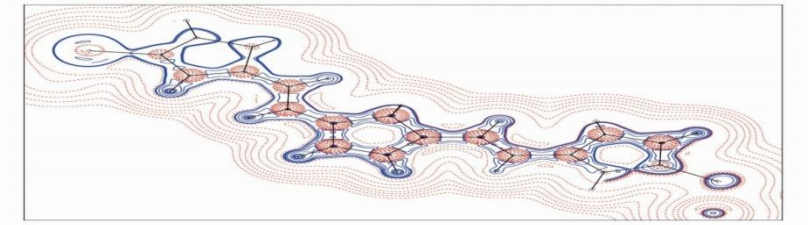
0.0	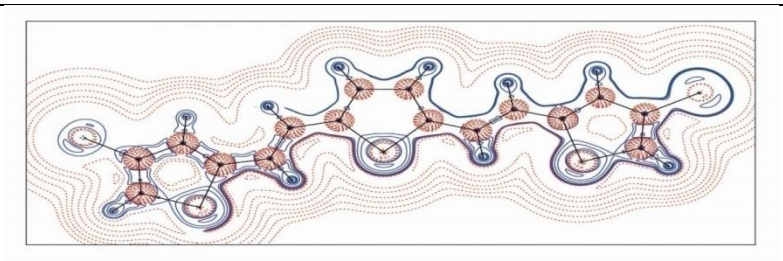
0.26	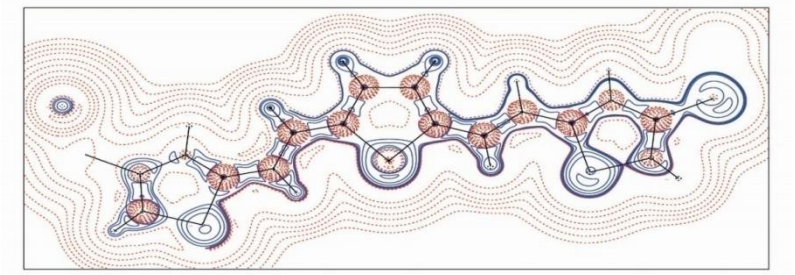

Fig. 6Laplacian of electron density map plotted for molecular plane of (a) diene and (b) phene for the zero and 0.26 applied Esther contours are drawn in logarithmic scale, $3x2^N$ $eÅ^{-5}$, where N = 2, 4 and $8x10^n$, n= -2, -1, 0, 1, 2. Solid lines are positive contours and dotted lines are negative contours

Table 2Laplacian of electron density values of the diene and phene wire for the various applied EFs (VÅ^{-1}).

Bonds	0	0.05	0.1	0.18	0.21	0.26
C (4)-C (3)	-19.791	-19.816	-19.829	-19.827	-19.772	-19.73
C (5)-C (4)	-11.76	-11.747	-11.739	-11.735	-11.739	-11.759
C (1)-C (5)	-11.253	-11.261	-11.269	-11.28	-11.298	-11.307
C (1)-C (2)	-19.739	-19.776	-19.793	-19.788	-19.765	-19.71
C (2)-C (3)	-14.249	-14.243	-14.255	-14.283	-14.328	-14.392
C (6)-C (1)	-16.116	-16.128	-16.169	-16.239	-16.321	-16.444
C (7)-C (6)	-19.931	-19.947	-19.935	-19.889	-19.816	-19.713
C (8)-C (7)	-16.009	-16.007	-16.04	-16.109	-16.197	-16.339
C (9)-C (8)	-11.441	-11.453	-11.462	-11.465	-11.469	-11.476
C (10)-C (9)	-11.615	-11.62	-11.621	-11.617	-11.607	-11.601
C (10)-C (11)	-19.284	-19.275	-19.231	-19.153	-19.056	-18.925
C (11)-C (12)	-15.563	-15.583	-15.649	-15.764	-15.888	-16.06
C (12)-C (8)	-18.999	-18.983	-18.938	-18.864	-18.776	-18.65
C (13)-C (10)	-16.393	-16.444	-16.529	-16.644	-16.754	-16.882
C (14)-C (13)	-19.924	-19.875	-19.795	-19.684	-19.556	-19.415
C (15)-C (14)	-15.742	-15.762	-15.812	-15.887	-15.97	-16.072
C (16)-C (15)	-11.339	-11.316	-11.291	-11.263	-11.233	-11.202
C (17)-C (16)	-11.956	-11.934	-11.911	-11.882	-11.854	-11.859
C (18)-C (17)	-19.715	-19.686	-19.652	-19.617	-19.575	-19.553
C (18)-C (19)	-14.249	-14.238	-14.241	-14.254	-14.265	-14.267
C (19)-C (15)	-19.388	-19.331	-19.253	-19.159	-19.055	-18.933
C (3)-S (20)	-4.702	-4.676	-4.655	-4.643	-4.662	-4.674
S (21)-C (18)	-4.678	-4.679	-4.674	-4.66	-4.645	-4.629
S(20)-Au(22)	2.95	2.974	3.006	3.054	3.105	3.156
S(21)-Au(23)	2.941	2.947	2.963	2.988	3.031	3.068

Bonds	0	0.05	0.1	0.18	0.21	0.26
C(4)-C(3)	-18.768	-18.78	-18.784	-18.786	-18.789	-18.79
C(4)-S(32)	-5.399	-5.354	-5.33	-5.309	-5.255	-5.197
S(32)-C(1)	-4.329	-4.293	-4.245	-4.2	-4.167	-4.131
C(2)-C(1)	-18.81	-18.808	-18.795	-18.776	-18.753	-18.726
C(3)-C(2)	-15.704	-15.686	-15.668	-15.648	-15.642	-15.641
C(1)-C(5)	-15.722	-15.697	-15.676	-15.648	-15.632	-15.634
C(5)-C(6)	-20.157	-20.144	-20.122	-20.1	-20.062	-20.018
C(6)-C(7)	-15.68	-15.715	-15.758	-15.801	-15.848	-15.903
C(7)-C(10)	-18.162	-18.179	-18.187	-18.186	-18.179	-18.162
C(7)-S(31)	-4.671	-4.65	-4.63	-4.615	-4.589	-4.564
C(10)-C(9)	-16.88	-16.885	-16.897	-16.899	-16.922	-16.964
C(9)-C(8)	-18.35	-18.354	-18.351	-18.352	-18.342	-18.324
S(31)-C(8)	-4.749	-4.73	-4.71	-4.693	-4.665	-4.639
C(8)-C(11)	-15.919	-15.896	-15.881	-15.84	-15.832	-15.837
C(11)-C(12)	-20.152	-20.163	-20.165	-20.16	-20.152	-20.139
C(12)-C(13)	-15.471	-15.49	-15.515	-15.529	-15.56	-15.595
C(13)-C(16)	-18.512	-18.52	-18.525	-18.529	-18.527	-18.521
C(13)-S(33)	-4.419	-4.415	-4.405	-4.384	-4.371	-4.358
C(14)-C(15)	-18.652	-18.678	-18.7	-18.727	-18.737	-18.742
C(16)-C(15)	-15.737	-15.74	-15.744	-15.719	-15.723	-15.729
S(33)-C(14)	-5.533	-5.477	-5.423	-5.348	-5.298	-5.244
S(17)-C(3)	-4.526	-4.534	-4.523	-4.506	-4.471	-4.431
C(15)-S(18)	-4.521	-4.49	-4.462	-4.444	-4.418	-4.396
Au(19)-S(17)	2.965	2.97	2.975	2.987	3.018	3.032
S(18)-Au(20)	2.953	2.974	3.004	3.063	3.095	3.133

ENERGY DENSITY

The bond strength of the molecule has been investigated from the total energy density H(r). The variation of H(r) of all the bonds was clearly pictured out in the figure 5c. The positive Laplacian of electron density results the impact of the kinetic energy density, which drives the depletion of bond charge at the bond critical point; though the negative Laplacian points to the administration of potential energy density, and the localization of charges. The total energy density H(r) from potential energy density V(r) and the neighborhood kinetic energy density G(r) in the bonding region can be likened as $H(r) = G(r) + V(r)$[20]. The present examination reports that the G(r) is positive, V(r) is negative and the total energy density H(r) is negative, clearly V(r) is consistently leads in all cases. The negative total energy density H(r) of Au and S uncovers that the convergence of negative charges in the bonding regions[21]. The covalent characteristics single and double bond

carbons are well obvious fromthe high negative total energy density H(r) values, ~-1.34HÅ^{-3} and ~-1.70 HÅ^{-3} for C-C bonds and~-2.09 and ~-2.04 HÅ^{-3} for C=C bonds in diene and phene molecules; separately. At the point when the applied electric field is accelerated, the total energy density H(r) of S-C bonds of the diene and phene molecules decreased feebly from -0.668 to -0.667 HÅ^{-3} and -0.674 to -0.66HÅ^{-3}respectively. The ionic nature of Au-S bonds of both diene and phenemolecules, are well established from their less negative H(r) values. As the field builds, the H(r) values of Au-S bonds are almost same, and the values are ~-0.155HÅ^{-3} [diene] and ~-0.157 HÅ^{-3} [phene]. All in all, it is noticed that the variations in energy densities of the two edges of the molecule are not same; still they differ systematically in the right edge of the molecule and their values are listed in the table 3. Comparative trend was watched for phenemolecule. The deviation in Fig 5c scenes the sulfur atom substitution.

Table 3Total energy density H(r) (HÅ^{-3}) values of the diene and phene wire for the various applied EFs (VÅ^{-1}).

Bonds	0	0.05	0.1	0.18	0.21	0.26
C(4)-C(3)	-2.161	-2.164	-2.166	-2.166	-2.16	-2.154
C(5)-C(4)	-1.248	-1.248	-1.247	-1.246	-1.246	-1.248
C(1)-C(5)	-1.197	-1.199	-1.199	-1.201	-1.203	-1.204
C(1)-C(2)	-2.119	-2.122	-2.122	-2.12	-2.115	-2.107
C(2)-C(3)	-1.511	-1.507	-1.508	-1.508	-1.512	-1.517
C(6)-C(1)	-1.653	-1.653	-1.656	-1.663	-1.671	-1.684
C(7)-C(6)	-2.126	-2.128	-2.126	-2.119	-2.11	-2.095
C(8)-C(7)	-1.644	-1.644	-1.648	-1.656	-1.667	-1.683
C(9)-C(8)	-1.212	-1.213	-1.213	-1.213	-1.213	-1.213
C(10)-C(9)	-1.231	-1.232	-1.232	-1.232	-1.231	-1.23
C(10)-C(11)	-2.059	-2.057	-2.05	-2.04	-2.028	-2.011
C(11)-C(12)	-1.631	-1.633	-1.64	-1.652	-1.665	-1.683
C(12)-C(8)	-2.044	-2.043	-2.037	-2.028	-2.017	-2.001
C(13)-C(10)	-1.683	-1.688	-1.698	-1.71	-1.723	-1.739
C(14)-C(13)	-2.126	-2.12	-2.11	-2.097	-2.082	-2.065
C(15)-C(14)	-1.616	-1.62	-1.628	-1.638	-1.65	-1.663
C(16)-C(15)	-1.203	-1.201	-1.198	-1.195	-1.192	-1.189
C(17)-C(16)	-1.268	-1.267	-1.265	-1.262	-1.26	-1.26
C(18)-C(17)	-2.152	-2.15	-2.146	-2.143	-2.139	-2.136
C(18)-C(19)	-1.515	-1.515	-1.517	-1.52	-1.523	-1.525
C(19)-C(15)	-2.098	-2.093	-2.085	-2.074	-2.062	-2.048
C(3)-S(20)	-0.669	-0.668	-0.667	-0.669	-0.673	-0.676
S(21)-C(18)	-0.667	-0.666	-0.665	-0.665	-0.664	-0.664
S(20)-Au(22)	-0.156	-0.158	-0.158	-0.16	-0.159	-0.159
S(21)-Au(23)	-0.156	-0.155	-0.154	-0.152	-0.149	-0.145

Bonds	0	0.05	0.1	0.18	0.21	0.26
C(4)-C(3)	-2.069	-2.07	-2.07	-2.072	-2.072	-2.073
C(4)-S(32)	-0.737	-0.734	-0.731	-0.729	-0.724	-0.718
S(32)-C(1)	-0.63	-0.627	-0.622	-0.618	-0.615	-0.611
C(2)-C(1)	-2.061	-2.063	-2.062	-2.061	-2.059	-2.057
C(3)-C(2)	-1.666	-1.666	-1.665	-1.663	-1.664	-1.665
C(1)-C(5)	-1.632	-1.632	-1.632	-1.632	-1.632	-1.636
C(5)-C(6)	-2.164	-2.163	-2.161	-2.159	-2.154	-2.149
C(6)-C(7)	-1.627	-1.629	-1.632	-1.636	-1.64	-1.646
C(7)-C(10)	-1.993	-1.995	-1.996	-1.996	-1.994	-1.992
C(7)-S(31)	-0.661	-0.659	-0.657	-0.656	-0.653	-0.651
C(10)-C(9)	-1.776	-1.776	-1.776	-1.776	-1.778	-1.782
C(9)-C(8)	-1.996	-1.997	-1.997	-1.998	-1.998	-1.996
S(31)-C(8)	-0.672	-0.669	-0.668	-0.666	-0.664	-0.661
C(8)-C(11)	-1.653	-1.652	-1.651	-1.648	-1.648	-1.651
C(11)-C(12)	-2.165	-2.165	-2.165	-2.165	-2.164	-2.162
C(12)-C(13)	-1.606	-1.606	-1.607	-1.606	-1.608	-1.612
C(13)-C(16)	-2.044	-2.045	-2.046	-2.048	-2.047	-2.047
C(13)-S(33)	-0.637	-0.637	-0.636	-0.636	-0.634	-0.633
C(14)-C(15)	-2.054	-2.057	-2.061	-2.065	-2.068	-2.069
C(16)-C(15)	-1.676	-1.675	-1.674	-1.67	-1.67	-1.67
S(33)-C(14)	-0.751	-0.746	-0.74	-0.732	-0.728	-0.723
S(17)-C(3)	-0.656	-0.656	-0.655	-0.654	-0.649	-0.645
C(15)-S(18)	-0.655	-0.653	-0.651	-0.652	-0.652	-0.651
Au(19)-S(17)	-0.157	-0.157	-0.157	-0.157	-0.157	-0.157
S(18)-Au(20)	-0.157	-0.157	-0.157	-0.158	-0.158	-0.158

ATOMIC CHARGES

The basics of charge distribution of atoms is indispensable to perceive the reactivity, molecular electrostatic potential (MESP) and the electrostatic interactions [22,23]. The charge distribution of atoms has a huge commitment in ascertaining the electrical conductivity of a molecular framework. In this manner, to uncover all the charge related molecular properties, it is obligatory to break down the redistributed charges of atoms under zero and higher applied electric field. In the meantime, various calculations actualize distinctive system over the charge figuring; it is a starter factor to ascertain the electronic charges from different calculations. The atomic chargescalculated by Mulliken population analysis (MPA), which was compared against the normal

population analysis (NPA) charges. Among, charges determined from NPA conspire are trust worthy.

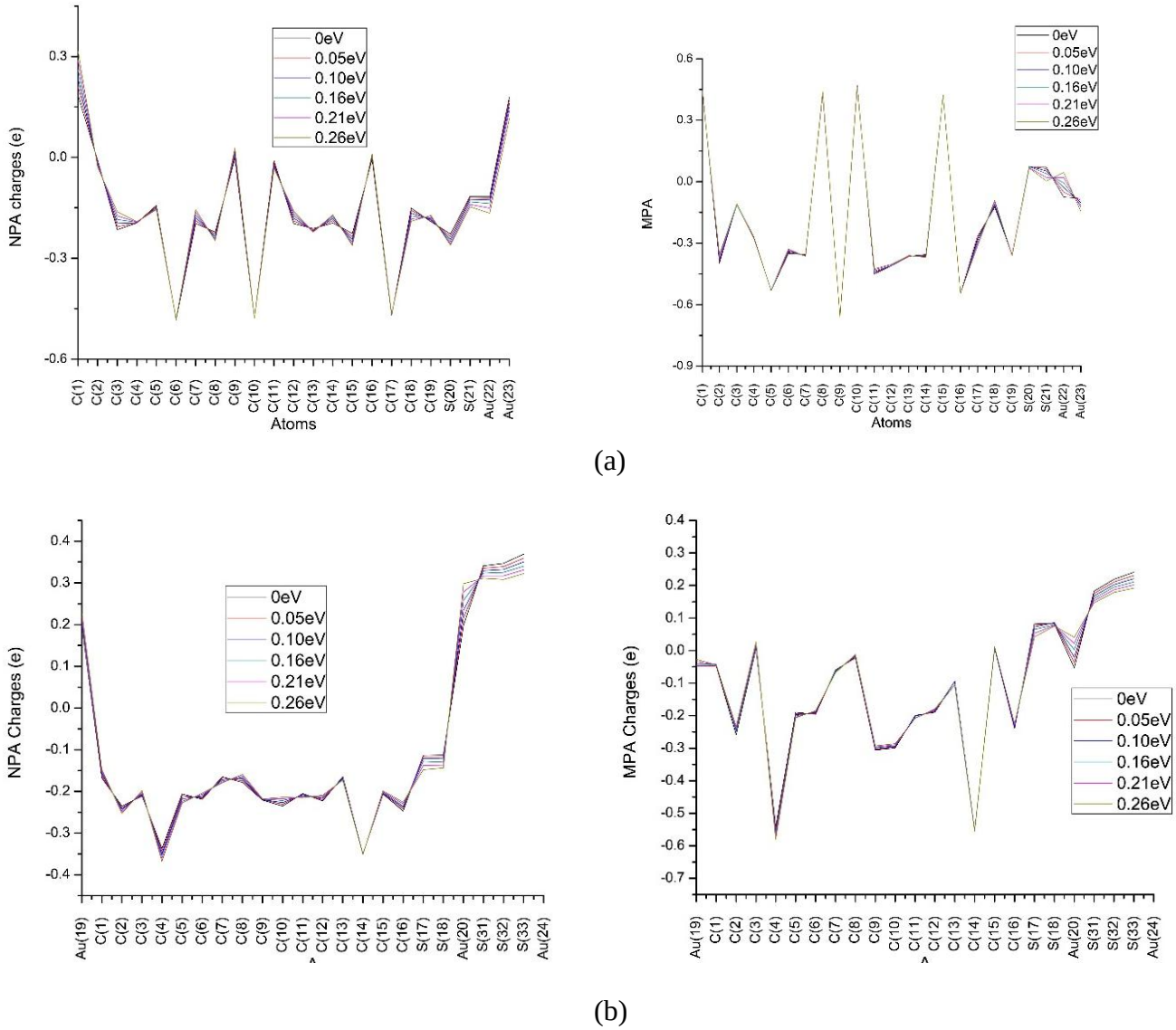

Fig. 7Variation of MPA and NPA charges of non-H atoms in (a) diene and (b) phene molecules calculated for various electric fields.

The charges of C(1), C(8), C(10) and C(15) atoms got from MPA conspire has high positive charge (~0.44e) for diene molecule, whereas in phene molecule, the high positive MPA [~0.11e] was calculated for C(4) and C(15) atoms. The normal estimation of MPA charges of S-atoms on the two edges for zero electric field is 0.07e [diene] and 0.08e [phene] respectively. At the point when the applied electric field is expanded from0eV, this value appears to be decreased to ~0.2 [diene] and ~0.01[phene] in both leftand right areas of the molecule. The MPA charges of Au atom ranges from -0.07 to 0.045e [diene] and - 0.046 to -0.027e [phene] for the increase of the applied electric field in the left end, while in the right end, the charges ranges from -0.08 to -0.145e [diene] and -0.053 to 0.041e [phene] when the applied electric field increments. The charge of all C-and S-atoms in the

electrode region from NPA plot appears to be negative. At the point when the electric field at the left end accelerated from 0 to 0.26VÅ^{-1}, the NPA charge of Au-atom have positive charge ranges from 0.18 to 0.21e [diene] and 0.22 to 0.27e [phene]. Figure.7 shows the clear picture of variation of MPA and NPA charges of diene and phene molecules for the various applied electric field.

FRONTIER MOLECULAR ORBITAL ANALYSIS

The energy gap between the highest occupied molecular orbital (HOMO) and lowest unoccupied molecular orbital (LUMO) is known as HOMO-LUMO gap (HLG), which directs the charge transport properties of the molecular nano wire. Henceforth, it is vital to examine the alterations in HOMO-LUMO gap and molecular orbital energy levels[24,26]for the applied electric fields. Fig. 8 depicts the variation of HLG for the zero and non-zero bias of molecular wire. The applied electric field significantly point out the frontier orbital energy levels of the system which are varied from each other and are predominantly symmetric for the reverse field effect. The external applied electric field made large differences in the distribution of orbitals. When the field increased from0 to 0.26VÅ^{-1}, there is sharp decrement in HOMO-LUMO gap from 1.297 to 0.648 eV for diene and from 1.672 to 1.085 eV for phene molecule [fig 8]. The HOMO and LUMO surface for 0 and 0.26 eV was shown in the figure 10.

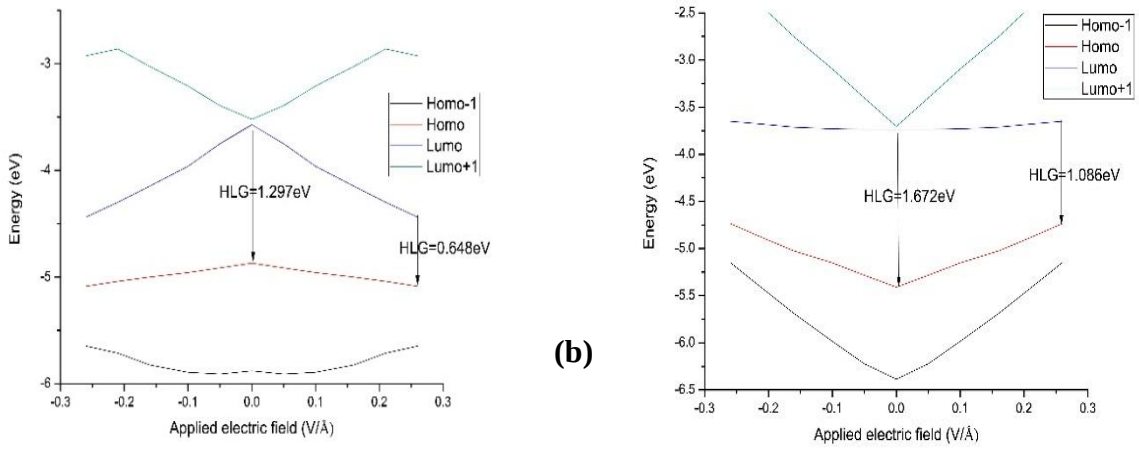

Fig. 8Variation of HLG for the various applied EFs in (a) diene and (b) Phene.

Fig. 9 explains the spatial redistribution of the molecular orbital for the zero and higher applied electric fields of the both diene and phene molecule.

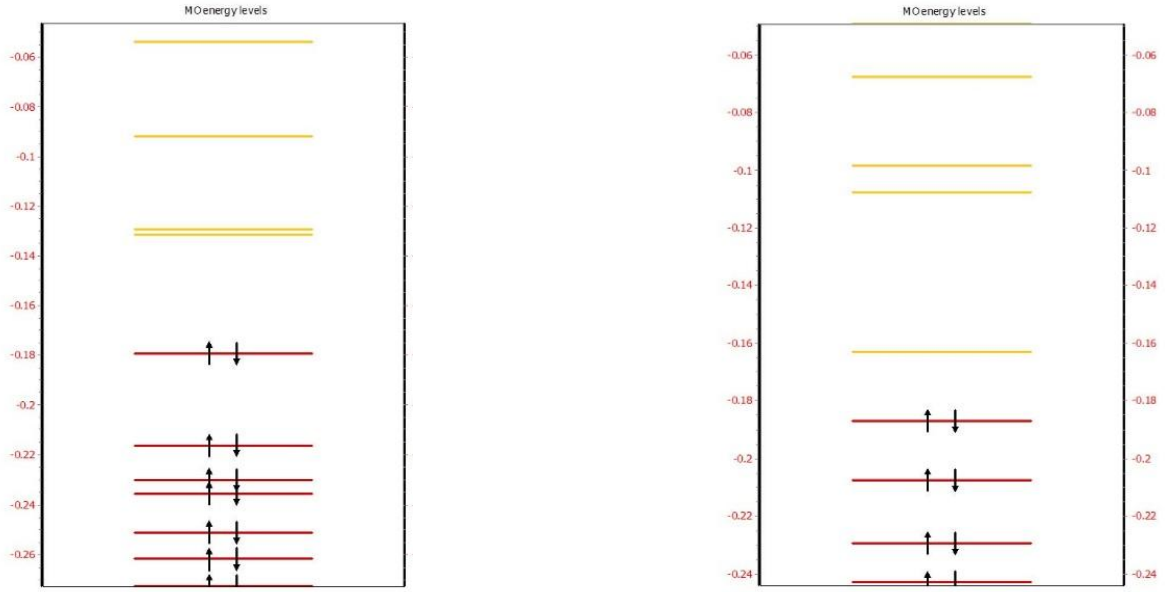

oeV 0.26eV

(a)

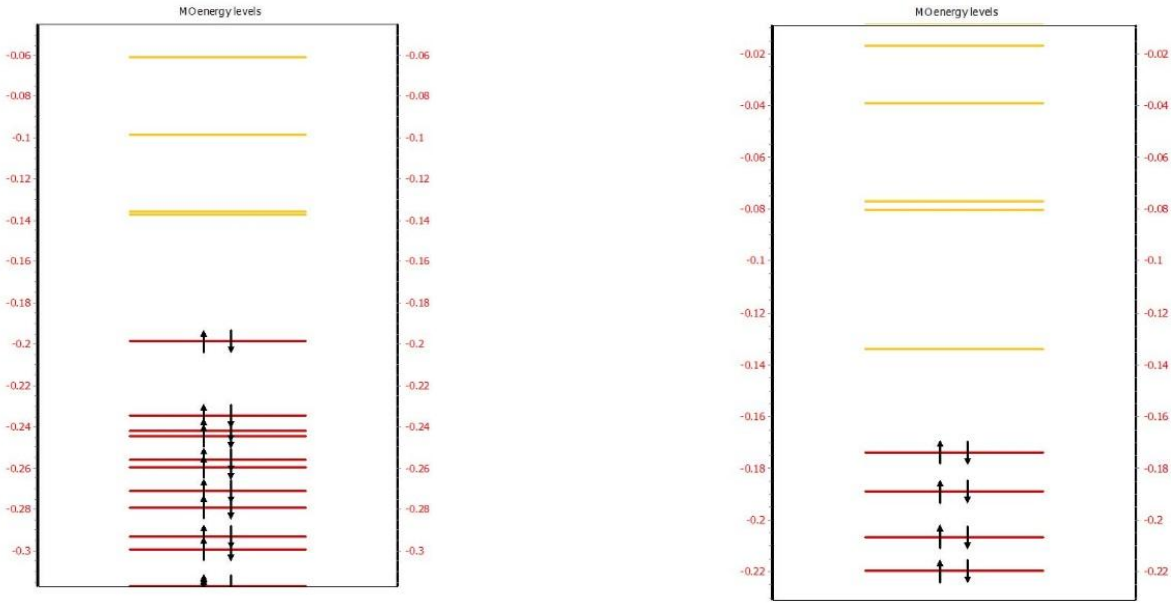

oeV 0.26eV

(b)

Fig. 9MO energy level of (a)diene and (b) Phene 0 and 0.26eV

HOMO

EF(VÅ^{-1})	DIENE	PHENE
0	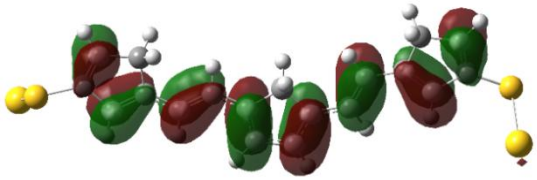	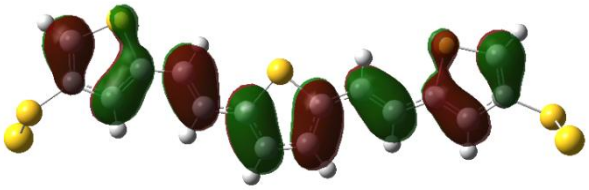
0.26	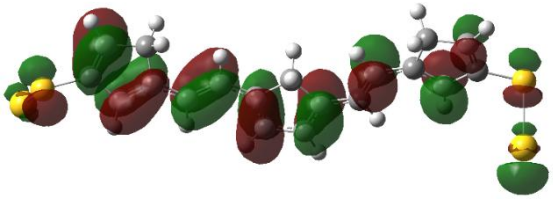	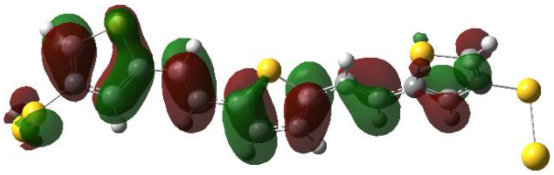

LUMO

EF(VÅ^{-1})	DIENE	PHENE
0	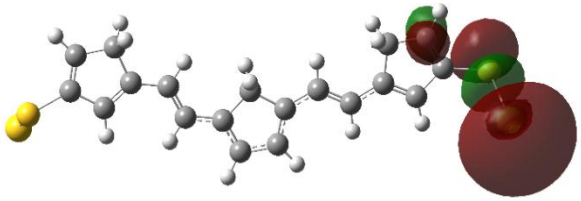	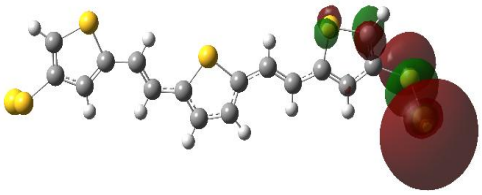
0.26	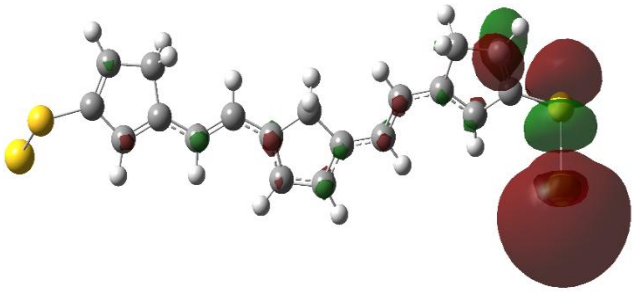	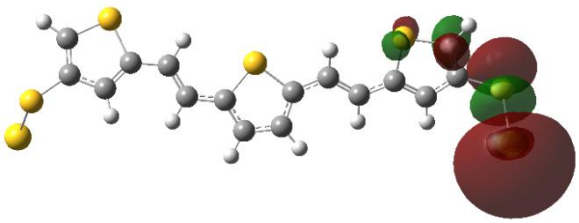

Fig. 10Isosurface representation of molecular orbital's (HOMO, LUMO) diene and phene for the zero and various applied EFs, which are drawn at 0.05au surface values.

ELECTROSTATIC POTENTIAL

Gadre and colleagues[27] revealed before that the plotting of iso-surface of the electrostatic potential (ESP) is a compact method to explore the chemical reactivity and electrostatic property of a molecule. One of the key utilizations of this work is the molecular electrostatic potential (MESP) came about because of the charge dissemination which permits to find the high electronegative and electropositive areas. Fig. 11 shows the three-dimensional iso-surface portrayals of electrostatic potential for the diene and phene molecule under zero and electric field. Here, blue surface signifies positive potential and red region symbolizes negative potential. The surface potential obviously replicates the opposing influences from the nuclei and the electrons, therefore it highly portraited the charged sections of the molecule.

The surface is seen as positive everywhere throughout the foundation of the molecule for the zero applied electric field; this positive impact is qualified from the nuclei. While, the negative potential is mounted over Sulphuratoms present at both edges of the molecule; this circumstance is almost same, when the field gets raised from 0 to 0.26VÅ^{-1}. Further, the balance parameter[28]was calculated for diene and phene molecules to explicit the exact composition of positive and negative potential. The balance parameter reaches a maximum value 0.25, when $\sigma^2(+)=\sigma^2(-)$. Here, we have calculated the positive and negative electrostatic potential variances and the electrostatic balance parameter listed in table 4 and the variation of balance parameter with the electric fields are shown in the figure 12.]

Table 4: Variance and balance parameter of diene and phene for various applied electric fields.

Diene

EF(VÅ^{-1})	$\sigma^2(+)$	$\sigma^2(-)$	Balance parameter
0	49.7	33.5	0.241
0.05	51.6	38.2	0.244
0.10	0.2	0.0	0.001
0.16	0.2	0.0	0.001
0.21	0.0	0.0	0.250
0.26	121.0	127.0	0.250

Phene

EF(VÅ^{-1})	$\sigma^2(+)$	$\sigma^2(-)$	Balance Parameter
0	78.61	18.92	0.156
0.05	0.00	0.00	0.149
0.10	3.68	0.00	0.000
0.16	2.88	0.00	0.000
0.21	0.14	0.00	0.000
0.26	130.45	33.41	0.162

EF(VÅ^{-1})	DIENE	PHENE
0	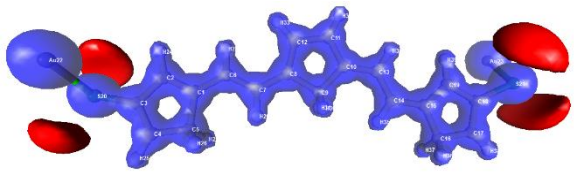	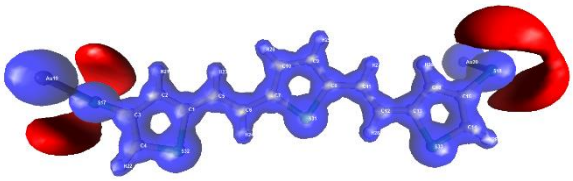
0.26	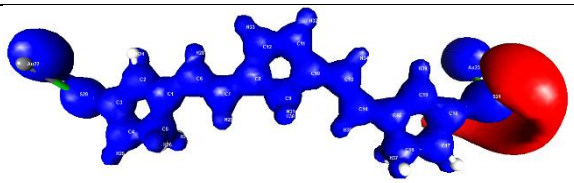	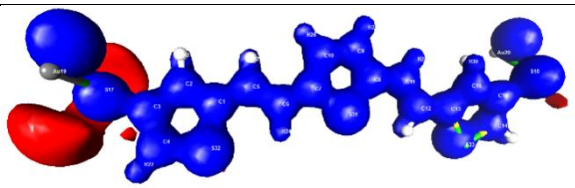

Fig. 11Isosurface representation of ESP of Au and S substituteddiene and phene for EFs 0 and 0.26eV. Blue: positive potential (0.5 eÅ^{-1}), Red: negative potential (-0.04 eÅ^{-1}).

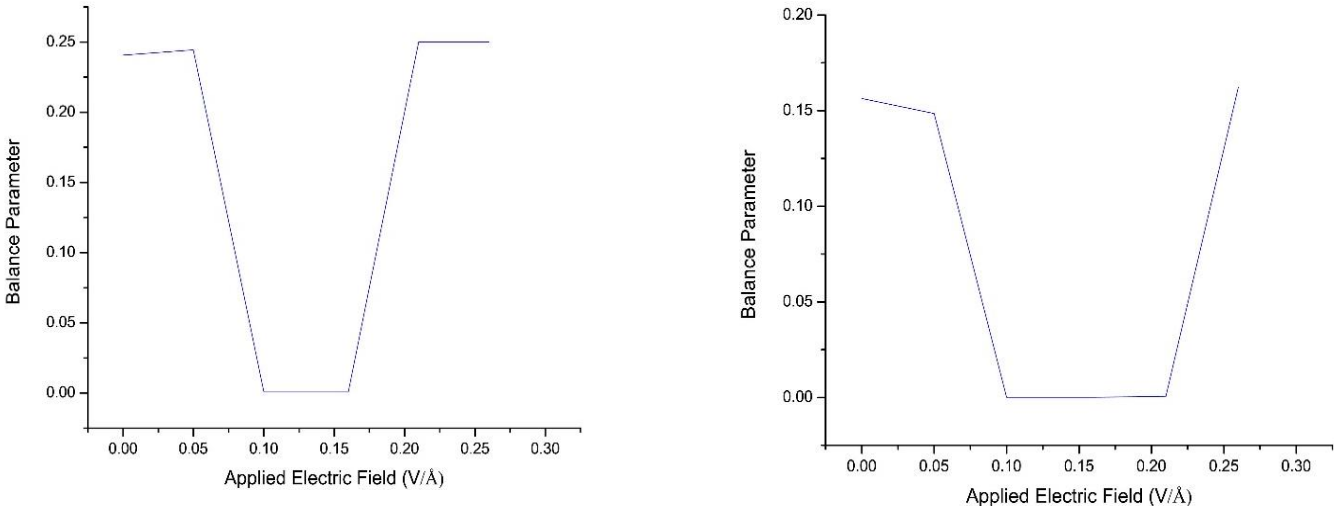

(a) (b)

Fig 12Variation of balance parameterfor the zero and various applied EF of (a) diene and (b) phene molecule

I-V RELATION AND MOLECULAR POLARIZATION

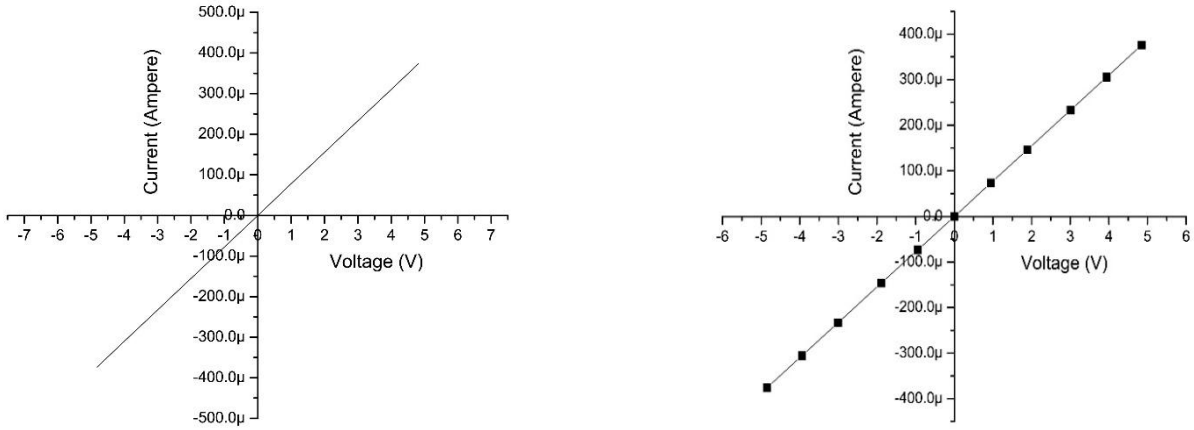

(a) (b)

Fig 13I-V characteristics plot of Au and S substitute (a) diene and (b) phenefor the zero and various applied EFs

The current–voltage (I–V) characteristic curve generally used to determine the basic parameters of electronic devices[29].The I-V characteristic plot [Figure 13] of the Au and S substituted diene and phene shows that, as the bias voltage increases, the current increases gradually showing the almost linear behavior of the molecule.

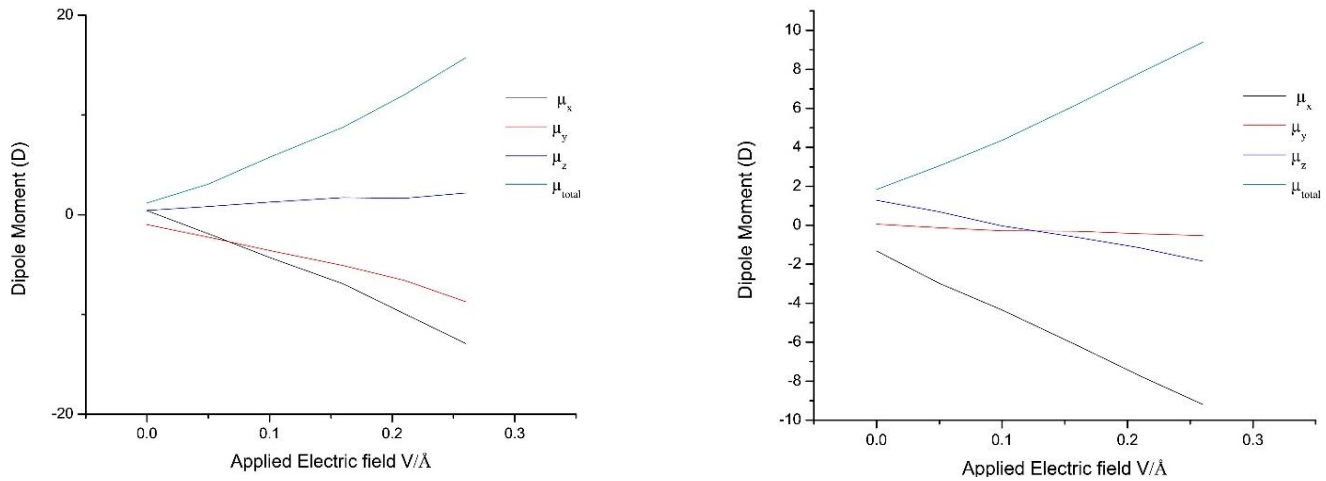

(a) (b)

Fig 14Molecular dipole moment of Au and S substituted (a) diene and (b) phene

The external EF field polarizes the molecule, which leads to change the dipole moment of the molecule. Hence, it is necessary to find out the dipole moment of the molecule for various applied EFs. The variations of molecular dipole moment for the various applied EF were analyzed by Kirtman et al., [30]and found a linear character. The molecule found to be highly polarized at the zero field.The Fig. 14 shows the variation of x, y and z components of dipole moment (μ_x, μ_y, and μ_z) and the resultant molecular dipole moment (μ) for various applied EFs, the large variation of x-component may be due to the application of field along x-direction.

CONCLUSION

The topological electron density and the electrostatic properties of diene and phene fused between electrodes were anticipated from QTAIM investigation for different applied electric fields. The geometrically minimized structures for zero and higher applied electric fields were obtained from the DFT estimations. The electron density investigation of the molecules shows the charge dispersion in all covalent and non-covalent bonds. At the point when the applied electric field is expanded, the HLG of the molecule varies significantly. Hence, the results of the examination may consent to build the electronic devices by utilizing these molecular nanowires.

REFERENCES

1 Nitzan . A, Ratner.M.A, Electron transport in molecular wire junctions, Science. 2003, 300(5624), 1384-1389.

2 Bader.R.F.W, A Quantum Theory of Molecular Structure and Its Applications, Chem. Rev. 1991, 91 (5), 893-928.

3 Geerlings. P, De Proft. F, Langenaeker. W, Conceptual Density Functional Theory, Chem. Rev. 2003, 103 (5), 1793-1873.

4 Frisch. M.J, Trucks. G.W, Schlegel. H.B, Scuseria. G.E, Robb. M.A, Cheeseman. J.R, Scalmani.G, Barone. V, Mennucci. B, Petersson. G.A, Nakatsuji. H, Caricato. M, Li. X, Hratchian. H.P, Izmaylov. A.F, Bloino. J, Zheng. G, Sonnenberg. J.L, Hada. M, Ehara. M, Toyota. K, Fukuda. R, Hasegawa. J, Ishida. M, Nakajima. T, Honda. Y, Kitao. O, Nakai. H, Vreven. T, Montgomery Jr.J.A, Peralta. J.E, Ogliaro. F, Bearpark. M, Heyd. J.J, Brothers. E, Kudin. K.N, Staroverov. V.N, Kobayashi. R, Normand. J, Raghavachari. K, Rendell. A, Burant. J.C, Iyengar. S.S, Tomasi. J, Cossi. M, Rega. N, Millam. J.M, Klene. M, Knox. J.E, Cross. J.B, Bakken. V, Adamo. C, Jaramillo. J, Gomperts. R, Stratmann. R.E, Yazyev. O, Austin. A.J, Cammi. R, Pomelli. C, Ochterski. J.W, Martin. R.L, Morokuma. K, Zakrzewski. V.G, Voth. G.A, Salvador. P, Dannenberg. J.J, Dapprich. S, Daniels. A.D, Farkas, Foresman. J.B, Ortiz. J. V, Cioslowski. J, Fox. D.J, Gaussian09 Revision D.01, Gaussian Inc. Wallingford CT, Gaussian 09 Revis. C.01. 2010.

5 Becke. A.D, Density-functional exchange-energy approximation with correct asymptotic behavior, Phys. Rev. A. 1988, 38 (6), 3098-3100.

6 Check. C.E, Faust. T.O, Bailey. J.M, Wright, B.J, Gilbert. T.M, Sunderlin. L.S, Addition of polarization and diffuse functions to the LANL2DZ basis set for P-block elements, J. Phys. Chem. A. 2001, 105 (34), 8111-8116.

7 Chiodo. S, Russo. N, Sicilia. E, LANL2DZ basis sets recontracted in the framework of density

functional theory, J. Chem. Phys. 2006, 125 (10), 104107.
8 Carbó-Dorca. R, Bultinck. P, Quantum mechanical basis for Mulliken population analysis, J. Math. Chem. 2004, 36 (3), 231-239.
9 Reed. A.E, Weinstock. R.B, Weinhold. F, Natural population analysis, J. Chem. Phys. 1985, 83, 735.
10 König. F.B, Schönbohm. J, Bayles. D, AIM2000-a program to analyze and visualize atoms in molecules, J. Comput. Chem. 2001, 22 (5), 545-559.
11 Volkov. A, Koritsanszky. T, Chodkiewicz. M, King. H.F, On the basis-set dependence of local and integrated electron density properties: Application of a new computer program for quantum-chemical density analysis, J. Comput. Chem. 2009, 30, 1379-1391.
12 Koritsanszky. T, Macchi. P, Gatti. C, Farrugia. L, Mallison. P.R, Volkov. A, Richter. T, XD2006. A computer program package for multipole refinement and analysis of charge densities from diffraction data., 2006.
13 Petkau. A, Stuart-Edwards. M, Stothard. P, Van Domselaar. G, Interactive microbial genome visualization with GView, Bioinformatics. 2010, 26, 3125.
14 N.M.O'Boyle, Tenderholt. A.L, Langner. K.M, Cclib: A library for package-independent computational chemistry algorithms, J. Comput. Chem. 2008, 29, 839-845.
15 Bulat. F.A, Toro-Labbé. A, Brinck. T, Murray. J.S, Politzer. P, Quantitative analysis of molecular surfaces: Areas, volumes, electrostatic potentials and average local ionization energies, in: J. Mol. Model., 2010, 11, 1679-1691.
16 Kutzelnigg. W, Atoms in Molecules. A Quantum Theory. (Reihe: International Series of Monographs on Chemistry, Vol. 22.) Von R.F.W. Bader. Clarendon Press, Oxford, 1990. XVIII, 438 S., geb. £ 50.00. – ISBN 0-19-855168-1, Angew. Chemie. 1992, 104, 1423.
17 Gibbs. G. V, Tamada. O, Boisen. M.B, Hill. F.C, Laplacian and bond critical point properties of the electron density distributions of sulfide bonds; a comparison with oxide bonds, Am. Mineral. 1999, 84, 435–446.
18 Amos. R.D, Andrews. J.S, Handy. N.C, Knowles. P.J, Open-shell MØ ller-Plesset perturbation theory, Chem. Phys. Lett. 1991, 185 (3), 256-864.
19 Lang. N.D, Interaction between closed-shell systems and metal surfaces, Phys. Rev. Lett. 1981, 46, 842.
20 Cremer. D, Kraka. E, Chemical Bonds without Bonding Electron Density — Does the Difference Electron-Density Analysis Suffice for a Description of the Chemical Bond?, Angew. Chemie Int. Ed. English. 1984, 23 (8), 627-628.
21 CremerD, Kraka. E, A Description of the Chemical Bond in Terms of Local Properties of Electron Density and Energy, Croat. Chem. Acta. 1984, 57, 1259-1281.
22 Molecular Electrostatic Potentials - Concepts and Applications, Theor. Comput. Chem. 1996, 3, 1-665.
23 Murray. J.S, Politzer. P, The electrostatic potential: An overview, Wiley Interdiscip. Rev. Comput. Mol. Sci. 2011, 1, 153-163.
24 Kim. B.G, Ma. X, Chen. C, Ie. Y, Coir. E.W, Hashemi. H, Aso. Y, Green. P.F, Kieffer. J, Kim. J, Energy level modulation of HOMO, LUMO, and band-gap in conjugated polymers for organic photovoltaic applications, Adv. Funct. Mater. 2013.
25 Perepichka. D.F, Bryce. M.R, Molecules with exceptionally small HOMO-LUMO gaps, Angew. Chemie - Int. Ed. 2005.
26 Ruiz-Morales. Y, HOMO-LUMO gap as an index of molecular size and structure for polycyclic aromatic hydrocarbons (PAHs) and asphaltenes: A theoretical study. I, J. Phys. Chem. A. 2002, 106 (46), 11283-11308.
27 Gadre. S.R, Pathak. R.K, Nonexistence of local maxima in molecular electrostatic potential maps, Proc. Indian Acad. Sci. - Chem. Sci. 1990, 102, 189-192.
28 Murray. J.S, Politzer. P, Statistical analysis of the molecular surface electrostatic potential: An

approach to describing noncovalent interactions in condensed phases, J. Mol. Struct. THEOCHEM. 1998, 425, 107-114.

29 Mujica. V, Ratner. M.A, Current-voltage characteristics of tunneling molecular junctions for off-resonance injection, Chem. Phys. 2001, 264 (3), 365-370.

30 Kirtman. B, Champagne. B, Bishop. D.M, Electric field simulation of substituents in donor - Acceptor polyenes: A comparison with ab initio predictions for dipole moments, polarizabilities, and hyperpolarizabilities, J. Am. Chem. Soc. 2000, 122 (33), 8007-8012.